

PDF hosted at the Radboud Repository of the Radboud University Nijmegen

The following full text is a preprint version which may differ from the publisher's version.

For additional information about this publication click this link.

<http://hdl.handle.net/2066/83800>

Please be advised that this information was generated on 2017-12-06 and may be subject to change.

Theory of optically forbidden d-d transitions in strongly correlated crystals

M I Katsnelson¹ and A I Lichtenstein²

¹*Radboud University of Nijmegen, Institute for Molecules and Materials,
Heijendaalseweg 135, 6525 AJ Nijmegen, The Netherlands*

²*I. Institut für Theoretische Physik, Universität Hamburg,
Jungiusstraße 9, D-20355 Hamburg, Germany*

(Dated: September 1, 2010)

Abstract

A general multiband formulation of linear and non-linear optical response functions for realistic models of correlated crystals is presented. Dipole forbidden d-d optical transitions originate from the vertex functions, which we consider assuming locality of irreducible four-leg vertex. The unified formulation for second- and third-order response functions in terms of the three-leg vertex is suitable for practical calculations in solids. We illustrate the general approach by consideration of intraatomic spin-flip contributions, with the energy of $2J$, where J is a Hund exchange, in the simplest two-orbital model.

From the physical point of view the most of natural mineral dyes are the Mott or charge-transfer insulators and their colors are determined essentially by correlation effects¹. If a material has no energy gap or its value is smaller than the energy of visual light, it will be non-transparent, a black one or with metallic shine. In the case of broad-gap materials the absorption of visual light is determined by impurities (ruby, that is, Al₂O₃ doped with Cr³⁺ ions is a prototype example¹) or by optically (dipole) forbidden d-d transitions between different terms and multiplets belonging to the same dⁿ-configurations of transition metal ions for a pure system. The latter processes are responsible for a green color of NiO² and blue color of most of the divalent copper insulating compounds³. These systems are usually colored and transparent and the transparency itself is a manifestation of dipole-forbidden character of relevant optical transitions.

Up to now the optical properties of Mott or charge transfer insulators are considered within the framework of cluster approaches^{4,5}. The present paper develops a general translationally invariant formalism to treat the d-d transitions in strongly correlated *crystals*. It is commonly accepted now that the standard LDA(GGA) approach is insufficient to describe the electronic structure of the Mott insulators⁶. To have more adequate picture of single-electron spectra various approaches have been applied to the problem such as LDA+U⁷, self-interaction corrections⁸ and the GW-scheme⁹. However, all these approaches do not provide the correct atomic limit and in particular do not take into account the term and multiplet structure, which is crucial for optics. This problem can be solved within the LDA+DMFT (dynamical mean-field theory)^{10,11} and the Hubbard-I approximation^{11,12}. There were several attempts to calculate the optical properties within the LDA+DMFT using the Kubo formula for optical conductivity¹³⁻¹⁵. However, in all these calculations the vertex contributions were not taken into account and the two-particle Green functions were calculated as a convolution of two single-particle Green functions (for review of the LDA+DMFT see¹⁶). The latter contains only transitions related to the promotion of d-electrons to the p-band with the change of transition-metal configurations from dⁿ to d^{n±1} and thus this approach is not sufficient to explain why NiO is green.

In the DMFT approach the self-energy is local which leads to a cancellation of vertex corrections in the single-band Hubbard model¹⁷. However, this is not the case for a generic multiband situation, similar to a treatment of optical properties of disordered alloys in the coherent-potential approximation (CPA)¹⁸. Here we present the corresponding formulation

for linear and non-linear optical response functions.

We start with the general expression for linear optical conductivity

$$\sigma_{ab}(i\omega) = \frac{e^2}{\omega} T^2 \sum_{\nu\nu'} \sum_{1234} \langle 4 | v_a | 1 \rangle \langle 2 | v_b | 3 \rangle \chi_{1234}(i\nu, i\nu', i\omega) \quad (1)$$

where χ_{1234} is a generalized susceptibility in a quasiatomic basis set $|1\rangle = |iL\sigma\rangle$, where i, L, σ label sites, orbital quantum numbers and spin projections, respectively, v_a is the electron velocity operator ($a = x, y, z$), and we use the Matsubara Green functions; at the end of calculations the analytical continuation $i\omega \rightarrow \omega + i0$ should be performed¹⁹.

The two-particle Green function $\hat{\chi}$ is expressed in terms of the single-particle Green function \hat{G} and the irreducible vertex function $\hat{\Gamma}$ as^{17,20}:

$$\begin{aligned} \chi_{1234}(i\nu, i\nu', i\omega) &= -G_{12}(i\nu') G_{34}(i\nu) \delta_{\nu, \nu' + \omega} - \\ &- T \sum_{\nu''} \sum_{5678} G_{15}(i\nu') G_{84}(i\nu) \Gamma_{5678}(i\nu, i\nu'', i\omega) \chi_{6237}(i\nu'', i\nu', i\omega) \end{aligned} \quad (2)$$

which can be written in the matrix form in the fermionic Matsubara frequencies $(i\nu, i\nu')$ and the pairs of electron quantum numbers (14, 23) as

$$\hat{\chi} = \hat{\chi}_0 + \hat{\chi}_0 \hat{\Gamma} \hat{\chi} \quad (4)$$

where $\hat{\chi}_0 = -\hat{G} * \hat{G}$. Within the DMFT approximation the self-energy $\hat{\Sigma}(i\omega)$ is local, that is, diagonal in site indices and \mathbf{k} -independent in the momentum representation¹⁷. In addition we will assume a locality of the irreducible vertex function $\hat{\Gamma}$; this is the only approximation we add. Then, it can be obtained from the local version of Eq.(4):

$$\hat{\Gamma} = \hat{\chi}_{loc,0}^{-1} - \hat{\chi}_{loc}^{-1} \quad (5)$$

where $\hat{\chi}_{loc,0}, \hat{\chi}_{loc}$ are matrices in the Matsubara frequencies and pairs of orbital and spin indices, all site indices are supposed to be the same¹⁷. Both single-particle and two-particle *on-site* Green functions can be found numerically exactly using full diagonalization scheme²¹ or continuous-time Quantum Monte Carlo method²².

Thus, the optical conductivity (1) can be expressed in the following form:

$$\sigma_{ab}(i\omega) = -\frac{e^2}{\omega} T \sum_{\nu} \sum_{\mathbf{k}} \sum_{1234} \langle 4\mathbf{k} | v_a^{eff}(i\nu, i\omega) | 1\mathbf{k} \rangle G_{12}(\mathbf{k}, i\nu) \langle 2\mathbf{k} | v_b | 3\mathbf{k} \rangle G_{34}(\mathbf{k}, i\nu + i\omega) \quad (6)$$



Figure 1: (Color online) Diagrammatic representation of Eq.(6); thick lines are the exact Green functions, dot is the bare matrix element $\langle 1\mathbf{k}|v_a|2\mathbf{k}\rangle$ and dot with triangle corresponds to $\langle 1\mathbf{k}|v_a^{eff}(i\nu, i\omega)|2\mathbf{k}\rangle$.

where b1234) are orbital and spin indices only and the effective matrix element (three-leg vertex) satisfies the equation

$$\langle 4\mathbf{k}|v_a^{eff}(i\nu, i\omega)|1\mathbf{k}\rangle = \langle 4\mathbf{k}|v_a|1\mathbf{k}\rangle - T \sum_{\nu'} \sum_{\mathbf{k}'} \sum_{2356} \langle 3\mathbf{k}'|v_a^{eff}(i\nu', i\omega)|2\mathbf{k}'\rangle G_{25}(\mathbf{k}', i\nu') G_{63}(\mathbf{k}', i\nu' + i\omega) \Gamma_{5146}(i\nu', i\nu, i\omega) \quad (7)$$

Diagrammatically Eq.(6) is shown in Fig.1.

The effective matrix element $\langle 1\mathbf{k}|v_a^{eff}(i\nu, i\omega)|2\mathbf{k}\rangle$ is convenient since its use allows us to present the linear and non-linear response functions in the unified form. For example, the non-linear optical susceptibility describing a second harmonic generation can be *exactly* represented as a sum of diagrams shown in Figs.2a and 2b.

The corresponding analytical expression for Fig.2a reads

$$\chi_{abc}(i\omega, i\omega, 2i\omega) = \frac{e^2}{\omega^2} T \sum_{\nu} \sum_{\mathbf{k}} \sum_{123456} \langle 6\mathbf{k}|v_a^{eff}(i\nu, i\omega)|1\mathbf{k}\rangle G_{12}(\mathbf{k}, i\nu) \langle 2\mathbf{k}|v_b^{eff}(i\nu + i\omega, i\omega)|3\mathbf{k}\rangle G_{34}(\mathbf{k}, i\nu + i\omega) \langle 4\mathbf{k}|v_c^{eff}(i\nu - i\omega, 2i\omega)|5\mathbf{k}\rangle G_{56}(\mathbf{k}, i\nu - i\omega) \quad (8)$$

The calculations of magnetic susceptibility in the one-band Hubbard model²³ shows that the contributions of the six-leg vertex are small; one can hope that this is also the case for the second harmonic generations and thus Eq.(8) will be sufficient for real calculations.

We proceed with the multiband Hubbard model with the Hamiltonian

$$H = \sum_{i\mathbf{m}\sigma} \varepsilon_i c_{i\mathbf{m}\sigma}^{\dagger} c_{i\mathbf{m}\sigma} + \sum_{\substack{i \neq j \\ m m' \sigma}} t_{mm'}^{ij} c_{i\mathbf{m}\sigma}^{\dagger} c_{j\mathbf{m}'\sigma} + \frac{1}{2} \sum_{\substack{i\sigma\sigma' \\ m_1 m_2 m_3 m_4}} U_{m_1 m_2 m_3 m_4} c_{i\mathbf{m}_1\sigma}^{\dagger} c_{i\mathbf{m}_2\sigma'}^{\dagger} c_{i\mathbf{m}_4\sigma'} c_{i\mathbf{m}_3\sigma} \quad (9)$$

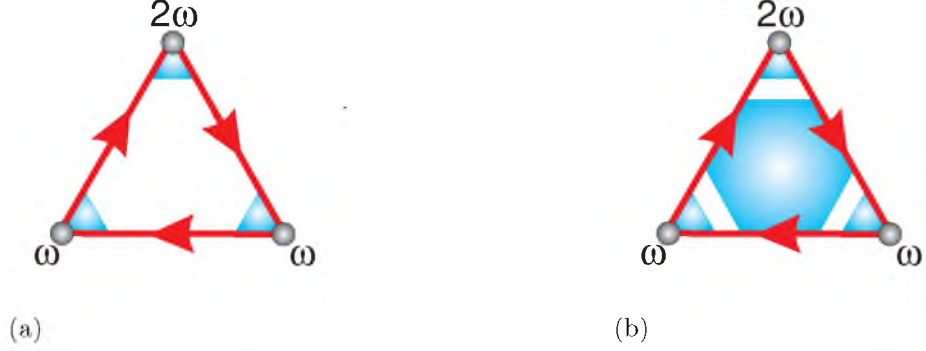


Figure 2: (Color online) Diagrammatic representation of the non-linear susceptibility for second harmonic generation; thick lines are the exact Green functions, dot with triangle corresponds to $\langle 1\mathbf{k} | v_a^{eff}(i\nu, i\omega) | 2\mathbf{k} \rangle$ and the shadowed hexagon is the irreducible six-leg vertex.

To clarify a physical meaning of vertex corrections to the response functions we discuss first exactly solvable model of two sites with two orbitals ($i = (1, 2)$, $m = (1, 2)$). The corresponding rotationally invariant interaction matrix is parametrized by the Hubbard energy U and the Hund exchange parameter J as²⁴

$$\begin{aligned}
 U_{m_1 m_1 m_1 m_1} &= U \\
 U_{m_1 m_2 m_1 m_2} &= U - 2J \\
 U_{m_1 m_2 m_2 m_1} &= J
 \end{aligned}
 \tag{10}$$

($m_1 \neq m_2$). The dimension of the Hilbert space is equal to 2^8 so $\hat{\chi}$ and \hat{G} can be easily found by exact diagonalization. The results for $\text{Im}\hat{\chi}/\omega \propto \text{Re}\hat{\sigma}(\omega)$ for real (not Matsubara) frequencies are shown in Fig.3 and Fig.4.

As one can see from the density of states the single-particle transitions which manifest themselves in $\hat{\chi}_0$ starts at the frequency $\omega \geq 1$ corresponding to the distance between the highest occupied and the lowest unoccupied orbitals. For small enough hopping (Fig.3a) there is a lot of peaks at smaller energies which originate from the poles of the vertex functions and represent the optically forbidden transitions in our toy model. In particular, a transition with $\omega = 2J = 0.4$ is clearly visible for intraband intersite transitions $(11) \rightarrow (21)$. The transition corresponds to local intraatomic spin flip processes. It is visible in optical (summed up over spins) susceptibility, since the Coulomb interaction matrix couples spin-up and spin-down states. An interesting and unexpected result of the toy model is that for a moderate hopping (Fig.3b) all these local term effects disappear.

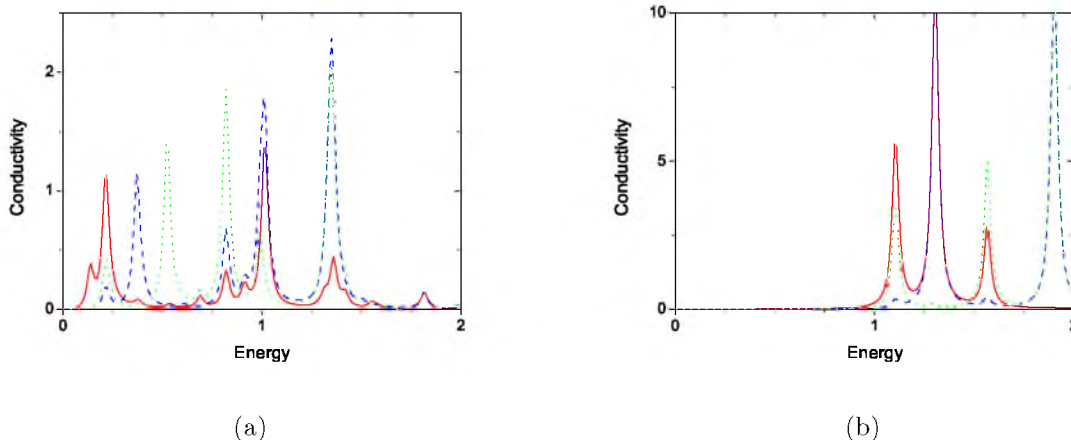


Figure 3: (Color online) Components of generalized susceptibility $\text{Im}\chi_{im,jm';im,jm'}/\omega$ summed up over (σ, σ') for two-site two-band model with $\varepsilon_1 = \varepsilon_2 = 0$, $U = 1$, $J = 0.2$, $t_{12} = t_{21} = 0.05$; (a): $t_{11} = t_{22} = 0.2$; (b) $t_{11} = t_{22} = 0.5$. Solid red curve corresponds to intrasite interband transitions $im = (11)$, $jm' = (12)$, dashed blue curve – to intersite intraband transitions $im = (11)$, $jm' = (21)$, and the dotted green curve – to intersite interband $im = (11)$, $jm' = (22)$. We use the spectral representation with the $\text{Im}\omega = 0.05$ and the temperature is $T = 0.05$. Energies are in the units of U .

Now we present the main part of our work related with the two-band lattice model with the use of local approximation for vertex $\hat{\Gamma}$ as describes above. The calculations have been done for the square lattice in the nearest neighbour approximation. The local vertex function has been obtained from Eq.(5) by exact diagonalization calculations of $\hat{\chi}$ and \hat{G} . If the exact diagonalization would be performed for intraatomic Coulomb interaction Hamiltonian only, this would correspond to the Hubbard I approximation¹¹. To go beyond this, in spirit of the DMFT¹⁷, we have added one more orbital to the bath.

Despite simplicity of the model our calculations turned out to be rather time and memory consuming due to the inversion of $\hat{\chi}$ -matrices depending of two Matsubara frequencies $(i\nu, i\nu')$. To reach convergence, we had to use about one hundred frequencies and 20×20 \mathbf{k} -points. The computational results are shown in Fig.5. One can see that $\hat{\chi}_0$ has only one pronounced peak at $\omega = U$ corresponding to the transition from the lower to upper Hubbard bands. At the same time, $\hat{\chi}$ has an additional peak within the gap of the single-particle excitation spectrum at the maximum around $\omega = 2J = 0.4$. This maximum originates from the spin-multiplet structure of the d^2 configuration.

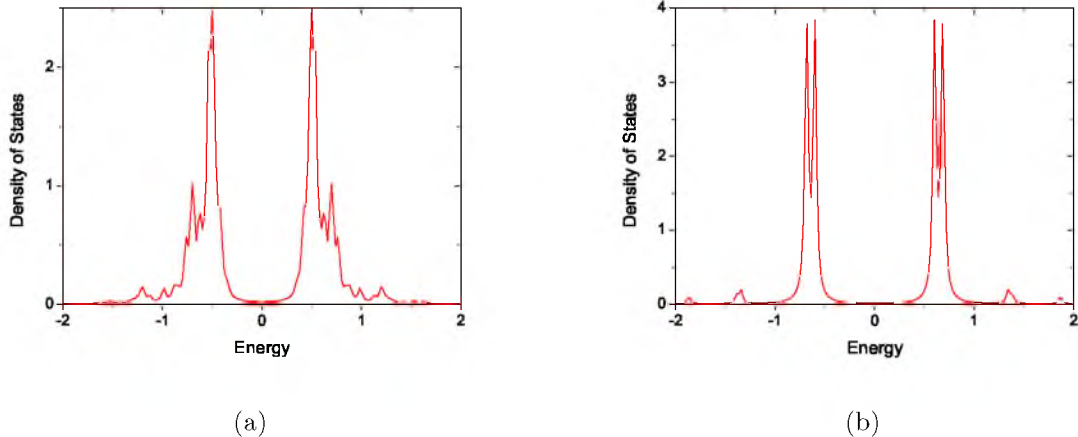


Figure 4: (Color online) Density of single-particle states for the same parameters as in Fig.3. Energies are in the units of U .

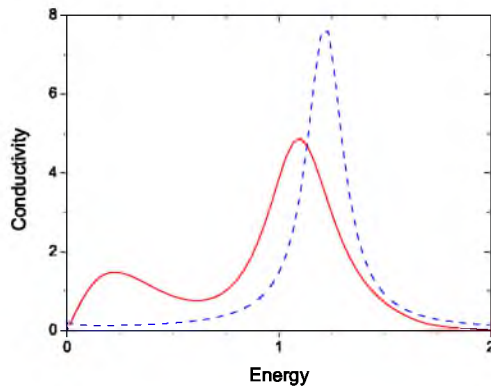


Figure 5: (Color online) Intrasite, interband components of $\text{Im}\hat{\chi}/\omega \propto \text{Re}\sigma(\omega)$ (solid red curve) and $\text{Im}\hat{\chi}_0/\omega \propto \text{Re}\sigma_0(\omega)$ (dashed blue curve) for the square lattice in the nearest-neighbour approximation, with the same parameters as in Fig.3a. Energies are in the units of U .

To conclude, we present a general formalism which allows to consider term and multiplet effects on linear and non-linear optical properties of multiband strongly correlated systems. For a two-band model the computational results are quite reasonable and one can hope that the scheme can be applied to the first-principle investigations of realistic systems in the spirit of the LDA+DMFT. The approach can be apply for other response functions such as magnetic susceptibilities and STM-spectroscopy where the transition with energy $\omega = 2J$ have been recently observed for Mn-chains on Pt surface²⁵.

-
- ¹ Sugano S, Tanabe Y and Kamimura H 1970 *Multiplets of Transition-Metal Ions in Crystals* (NY: Academic Press)
 - ² Fiebig M, Frhlich D, Lottermoser Th, Pavlov V V, Pisarev R V and Weber H-J 2001 *Phys. Rev. Lett.* **87**, 137202
 - ³ Pisarev R V, Sanger I, Petrakovskii G A and Fiebig M 2004 *Phys. Rev. Lett.* **93**, 037204
 - ⁴ Gossling A, Schmitz R, Roth H, Haverkort M W, Lorenz T, Mydosh J A, Muller-Hartmann E and Gruningen M 2008 *Phys. Rev. B* **78**, 075122
 - ⁵ Lin N, Gull E and Millis A J 2009 *Phys. Rev. B* **80**, 161105(R)
 - ⁶ Terakura K, Oguchi T, Williams A R and Kubler J 1984 *Phys. Rev. B* **30**, 4734
 - ⁷ Anisimov V I, Aryasetiawan F and Lichtenstein A I 1997 *J. Phys.: Condens. Matter* **9**, 767
 - ⁸ Svane A and Gunnarsson O 1990 *Phys. Rev. Lett.* **65**, 1148
 - ⁹ Faleev S V, van Schilfgaarde M and Kotani T 2004 *Phys. Rev. Lett.* **93**, 126406
 - ¹⁰ Anisimov V I, Poteryaev A I, Korotin M A, Anokhin A O and Kotliar G 1997 *J. Phys.: Condens. Matter* **9**, 7359
 - ¹¹ Lichtenstein A I and Katsnelson M I 1998 *Phys. Rev. B* **57**, 6884
 - ¹² Lebegue S, Santi G, Svane A, Bengone O, Katsnelson M I, Lichtenstein A I and Eriksson O 2005 *Phys. Rev. B* **72**, 245102
 - ¹³ Oudovenko V S, Palsson G, Savrasov S Y, Haule K and Kotliar G 2004 *Phys. Rev. B* **70**, 125112
 - ¹⁴ Chadov S, Minar J, Ebert H, Perlov A, Chioncel L, Katsnelson M I and Lichtenstein A I 2006 *Phys. Rev. B* **74**, 140411
 - ¹⁵ Windiks R, Wimmer E, Pourovskii L, Biermann S and Georges A 2008 *J. Alloys Compounds* **459**, 438
 - ¹⁶ Kotliar G, Savrasov S Y, Haule K, Oudovenko V S, Parcollet O and Marianetti C A 2006 *Rev. Mod. Phys.* **78**, 865
 - ¹⁷ Georges A, Kotliar G, Krauth W and Rozenberg M J 1996 *Rev. Mod. Phys.* **68**, 13
 - ¹⁸ Butler W H 1985 *Phys. Rev. B* **31**, 3260
 - ¹⁹ Mahan G D 2000 *Many-Particle Physics* (NY: Kluwer Academic/Plenum)
 - ²⁰ Migdal A B 1967 *Theory of Finite Fermi Systems and Applications to Atomic Nuclei* (NY: Wiley)

- ²¹ Hafermann H, Jung C, Brener S, Katsnelson M I, Rubtsov A N and Lichtenstein A I 2009 *EPL* **85**, 27007
- ²² Rubtsov A N, Katsnelson M I, Lichtenstein A I and Georges A 2009 *Phys. Rev. B* **79**, 045133
- ²³ Hafermann H, Li G, Rubtsov A N, Katsnelson M I, Lichtenstein A I and Monien H 2009 *Phys. Rev. Lett.* **102**, 206401
- ²⁴ Frèsard R and Kotliar G 1997 *Phys. Rev. B* **56**, 12909
- ²⁵ Hirjibehedin C F, Lutz C P and Heinrich A J 2006 *Science* **312**, 1021